ICAS PAPER

NO. 72 – 55

SOME RECENT DEVELOPMENTS IN THE UNDERSTANDING
OF ' JET NOISE '

by

J. D. Voce and J. Simson,
Bristol Engine Division Rolls–Royce (1971) Ltd.,
Bristol, U. K.

The Eighth Congress
of the
International Council of the
Aeronautical Sciences

INTERNATIONAAL CONGRESCENTRUM RAI-AMSTERDAM, THE NETHERLANDS
AUGUST 28 TO SEPTEMBER 2, 1972

Price: 3. Dfl.

Notice

Copies of figures   1.3, 1.4, 1.6, 1.7, 1.8, 1.11, 1.12, 3.3

may be obtained by direct application to

> J. Simoon
>
> Rolls Royce (1971) Ltd,
>
> P.O. Box 3,
>
> Filton, Bristol
>
> England

Some Recent Developments in the Understanding of Jet Noise

by

J.D. Voce and J. Simson

1.0 INTRODUCTION

Lighthill's treatment of the problem of aerodynamic noise (ref 1 and 2), which predicts a $(velocity)^8$ dependance for acoustic quadrupole sources, has been modified by Ffowcs Williams (ref 3 and 4) to take into account the effect of finite source volume and has been extended to supersonic convection speeds. He shows that the intensity of sound radiated in the direction of the Mach wave is dependent on the 3rd power of the velocity. Model tests carried out at Rolls-Royce tend to confirm Ffowcs Williams' theory although significant discrepancies occur at both high and low speeds increasing with angle to the jet.

The discrepancy at high speeds is associated with the shock structure of the supercritical jet. This problem can be solved by using a convergent-divergent nozzle but because of the practical problems involved in maintaining the nozzle design point other means of reducing or eliminating shock cells have been examined and are described in the paper. Also described are devices, other than convoluted or multi-tube type nozzles which attenuate jet mixing noise by inducing very rapid spread of the jet, which have been tested at Rolls-Royce.

JH

At low speeds the discrepancy has partly been explained by Hoch et al (ref.5) who has introduced a variable index to the density ratio in the normalising function. The remaining difference is considered to be due to other noise sources referred to as internal or tailpipe noise. Comparison of measurements made on a Rolls-Royce engine with those of its turbine in isolation suggests that at least part of this noise is generated upstream of the nozzle and this is substantiated by tests showing the effectiveness of acoustic absorbers and screens placed at the nozzle exit. However, screens could also be effective in modifying the disturbance caused by the nozzle lip on aerodynamic sources. Experiments have been carried out to modify these edge sources by changing the incident turbulence and it is shown that this has a significant effect on the spectra.

Finally the effect of forward speed on these sources is discussed. Tests are currently in hand on the Rolls-Royce spinning rig to investigate this effect further and will be reported at a later date.

SECTION 1. EXTERNALLY GENERATED NOISE

1.1. PURE JET NOISE

Lighthill (1) has treated the problem of aerodynamic noise sources using the now well known acoustic analogy, which predicts U^8 dependence for acoustic quadrupole sources whose strength is given by the turbulence stress tensor T_{ij}. Part II of the work (2) deals specifically with acoustic modelling of the jet by relating the theory to the statistical properties of the turbulent flow. Ffowcs Williams (3) has modified the amplification term $(1 - \epsilon M \cos \theta)^{-6}$ arising from the convection of quadrupole sources (1) to include the effect of finite source volume giving the acoustic intensity I:-

$$I \sim \frac{\rho^2}{\rho_0} \frac{U^8}{a_0^5} \left(\frac{D}{r}\right)^2 \frac{1}{(1 - \epsilon M \cos \theta)^5}$$

I is typical intensity

ρ exhaust gas density

$\rho_0 \ a_0$ ambient density and speed of sound

M Jet Mach No.

ϵ source convection factor

θ angle between observer and downstream jet axis

D nozzle diameter

r wave propagation distance

The singularity associated with $\epsilon M \cos \theta = 1$ and a general extension of the acoustic analogy to supersonic convection speeds is considered by Ffowcs Williams (4) where it is shown that the quadrupole sources break down into the constituent simple sources at this critical condition and are seen as high intensity waves on the eddy Mach cone. At super critical convection speeds, the simple sources are no longer heard independantly, giving the same quadrupole array, but now in

reverse time. Under these conditions $1-\epsilon M \cos\theta \longrightarrow \epsilon M \cos\theta$ as M increases giving a new velocity index to the Intensity dependence of 3 for sound radiated in the direction of the Mach wave.

The phenomena described in these references have been observed on tests at Rolls-Royce Bristol. Fig 1.1. A and B indicate the correlation of jet noise from model nozzles and engines at 45 and 105 degrees to the jet axis. The centre portion of the correlation compares very well with the Lighthill model, turning over to the lower U^3 velocity relation as predicted, but discrepancies begin to occur at the higher angle at supersonic jet velocity. At low velocity, the gradient of the line unexpectedly falls, indicating a divergence from the Lighthill model. Data for these curves is drawn from a variety of engine and model tests conducted at Rolls-Royce, but does not include the results from very clean model rigs which will be dealt with in a later section.

So it is seen that there are two major areas of discrepancy, each increasing with angle to the jet axis. The first is at low speed where the measured data is seen to peel off at lower gradient. This has partly been explained by Hoch et al (5) by introducing a variable index to the density ratio of the normalising function. However, there still remains a discrepancy which is considered to be the result of other noise sources which in general have a lower velocity index than for the convected quadrupole array. Further discussion will be given

to these sources in a later section on 'Internal" Noise sources.
The second discrepancy occurs at the high speed end of the
scale and is associated with the noise due to the shock structure
of the supersonic jet.

1.2 SHOCK CELL NOISE

Shock cell noise is always present in the over-
expanded jet where shocks are present. Two effects are observed
in the noise field, the first is a broad band noise component
and the second a more discrete phenomenon, but both are
considered to emanate from turbulence/shock interaction.
The discrete phenomenon, which is only in general observed on
cold jets is due to a feed back mechanism between the ends of
the shock cell and the nozzle lip or other reflecting surface
nearby, this screech mechanism is not considered important
at engine scale. However, the broad band component is an
important contributor to the noise field of engines at super-
critical pressure ratios as is seen by reference to fig.1.1.
it will also be seen (Section 3) that the problem becomes more
severe due to flight. Experimental evidence indicates that
the noise is of most practical importance in the forward arc
as shown in fig. 1.2.

The curves shown compare the linear acoustic field
shapes produced by both a properly expanded jet, achieved by
means of a con-di nozzle, and an over expanded jet from a simple
conical nozzle. Both jets are at a total temperature of $1100^{\circ}K$
and pressure ratio of 3.05:1. Shadowgraph flow visualisation

techniques clearly show the difference in the jet structure between these two cases. The conical nozzle flow is shown in fig. 1.3, where the shock cell structure may be clearly identified, whilst no shocks are distinguishable for the con-di nozzle flow given in fig.1.4.

Theoretical exploration of the phenomenon due to Fisher (6) treats the jet as an array of simple sources located near the shocks and excited by the passage of turbulence. The source array is amplitude and phase related by the shock cell dimension and the auto-correlation of the excitation turbulence, thus giving a far field spectrum and field directivity due to the multiple source intereference. The intensity of sound is seen to be proportional to the fourth power of the density discontinuity across the shock.

Spectral comparisons between the noise from the conical and con-di nozzles are shown in fig. 1.5., but it is not possible to see the predicted intereference character because of the logarithmic frequency scale that is used.

The con-di nozzle however does not easily lend itself to many practical applications where changes in operating conditions of the engine necessitate large geometry changes to keep on the nozzle design point. For shock noise reduction therefore, other devices to control the jet expansion have been investigated. A perforated shroud near the exit of a conical nozzle substantially removes the strong shocks as shown in the shadowgraph picture (Fig.1.6), the corresponding noise reduction for this configuration is compared with the conical and con-di results in fig.1.2. A further device of considerable interest is the

long slotted nozzle which is seen to produce a shock free
"fish tail" jet by controlling the jet expansion through the
narrow slot. The jet structure can be seen from shadowgraph
pictures from two perpendicular directions (Fig.1.7). Such
fish tail jets have good potential as jet noise silencers as
seen in the next section.

1.3. JET NOISE SILENCING

Much data has been published on various jet noise
silencers of the convoluted and multi-tube type which are well
known to give moderate attenuations. No more will be said
about such devices here. A subject which has not received so
much attention is the two dimensional or "fish tail" class
of jet silencers of which Rolls-Royce have some experience.

The object of the devices is to induce a very rapid
spread of the jet, in one plane, the quiet plane, with minimum
of thrust reduction. Rapid spreading with the associated high
eddy diffusivity induces a noise reduction in the plane of
fish tail which can be seen to reduce noise. For the high speed
jet, we have already seen that the intensity is proportional
to u^3, by dimensional analysis (7) we may write

$$\frac{K \alpha^2}{4\pi^2 r^2} \frac{\rho_i}{\rho_0} \rho_j \, u^4 G \, \tau$$

to represent the acoustic intensity for a single eddy in the
Mach wave direction.

where τ ~ eddy duration.

ρ_i ~ jet density

u ~ jet velocity

K ~ constant of proportionality

Now the number of eddies in volume V is $\qquad N \sim \dfrac{V}{D^2 c_0 \tau}$

where D is a dimension typical of the jet, giving a total intensity

per unit volume V for an observer at the Mach angle of

$$\frac{I}{V} \sim \frac{K \alpha^2}{4 \pi^2 r^2} \frac{\rho_j^2}{\rho_c} u^4 \frac{\tau}{D^2}$$

This formula indicates that noise reduction can be

achieved by increasing the typical eddy length scale, and

reducing the eddy life time. It is for this reason that asymmetric

nozzles inducing high eddy diffusivity are of great interest

for high speed jet noise reduction. A jet which has a high

eddy diffusivity is seen in fig 1.8 which shows shadowgraph

photographs in two perpendicular planes of the substantially

two-dimensional jet induced by convergent plates downstream of

a conical nozzle at pressure ratio of about 3:1. The spread

rate in the broad plane should be compared with the corresponding

conical nozzle flow shown in fig 1.3. or 1.4. Noise measurements

in both planes have shown that there is no substantial change

in peak noise with respect to the axisymmetric case normal to

the plane of the "fish tailed" jet, yet in the wide plane large

reductions are achieved as indicated in Fig. 1.9. The curve

compares the noise of the conical nozzle with that in the two

planes of the fish tail jet   as a function of angle 'Q' with

respect to the nozzle centreline. Subjective importance of the

phenomena is seen by presenting the noise as PNdB with respect

to peak noise from the conical nozzle. An indication of the

influence of plate contraction ratio is presented in fig.1.10

where peak to peak attenuations are plotted against a function

of plate convergence ratio which is a control of the jet spread

rate. Secondary deflector systems are however not the only way

of achieving high jet spread rates and eddy diffusivity. Other devices which exhibit the two-dimensional high spread rate phenomena are notched nozzles, a sketch of such a device is given in fig.1.11, whilst shadowgraphs of the resulting flow may be seen in fig. 1.12. Obvious similarities exist between this and fig. 1.8. for the corresponding squashed jet, similarities in the noise reduction also exist as may be seen from fig. 1.13 which is a field shape analogous to fig. 1.9.

SECTION 2

"INTERNAL" ON "TAILPIPE" NOISE SOURCES

"Internal noise" is the generic term used to describe the noise which forms the difference between the pure jet noise observed in the last section, and the noise of engines and many rigs. Examination of data from model jets and engines presented in fig.1.1. of the last section shows the divergence of predicted and measured noise as jet velocity becomes very low. This problem is most severe when engine data are considered in the correlation curves as shown in fig.2.1. which separates the best models from a mean line through the engine test points covered by Rolls-Royce in recent years. (For example see ref. 8). One source of discrepancy at high velocity, namely shock cell noise has already been discussed, now the aim is to investigate the nature of the discrepancy at the lower speed end of the scale.

Perhaps the best way to describe the problem is to take a particular example, in this case a twin spool turbojet engine operating at the lower end of its running line. Spectra plotted on a constant bandwidth format are presented in Fig. 2.2. for increasing engine power corresponding to points A,B,C and D on fig 2.1. Also shown are the estimated jet noise spectra for the two extreme cases, these data being extracted from the results obtained at model scale as outlined in section 1. One feature of the engine spectra that is not modelled is the ground reflection interference pattern due to the interaction of the direct signal with the signal reflected from the ground plane.

Taking the spectra in fig. 2.2. in turn from the lowest (A) one can observe the source of internal noise. At low velocity the tonal component due to the turbine is clearly seen, being dominated by the low pressure turbine tone (LPT). This tone has suffered considerable spectral broadening, a feature easily seen when comparison is made with the analyser filter shape which is shown on the figure. Also present are other tones at frequencies related to the difference between high and low pressure ratio turbine tones (HPT-LPT), yet the high pressure turbine tone is not self evident, the predicted frequency being about 9.4 KHz for conditions A. Evidence of harmonics of compressor tones (LPC) are also observed, all making a contribution to the total noise over and above the jet noise floor. As the jet velocity increases, this fine character of the spectrum becomes less significant and the broad band components become dominant in accounting for the tailpipe noise phenomena, until at condition D, the low frequency part of the spectrum is almost entirely accounted by jet noise. In each case however, the higher frequency is in excess of the jet noise. The other major characteristic of tailpipe noise is the tendency to peak at higher angles to the jet than pure jet noise, this may be seen by refering back to the overall correlations in fig.1.1. by observing the increased divergence of measured results at low U_j as 'θ' increases from the jet axis in fig 1.1.b.

Let us consider some possible mechanism for this additional noise which may help towards its elimination.

First consider noise sources contained within the jet
pipe. It is already seen from fig. 2.2 that discrete signals
due to turbine interaction tones are significant at low power
settings, but the energy contained is not suffucient to
explain all the tailpipe noise phenomena, particularly as the
jet velocity is increased as in C of 2.2. where new broad band
components obscure the discrete phenomena. This does not of
course rule out the broad band component due to the turbulence
interaction with the turbine blading, which becomes a very
strong contender as one would expect the principle acoustic
source terms to be dipole in nature and hence radiating
with intensity proportional to the sixth power of the
local velocity. Velocity indices of approximately 6 or below are
seen in the overall results, based on the fully expanded jet
velocity, but for subsonic jets this is simple related to
the jet pipe or any other internal velocity by the nozzle
contraction ratio. Experiments performed on an isolated turbine
illustrate this point when compared with the full engine. Fig. 2.3
shows noise plots from a Rolls-Royce turbine which was run over
a matrix of operating conditions in isolation from the engine.
The data are plotted as a jet noise correlation and are seen
to represent a band above the total jet noise of the full engine,
but the turbine rig used a large nozzle in order to keep jet
velocities low during the investigation, and it is only when
the data are effectively replotted against jet pipe velocity
that the rig and engine results line up. This is effectively
done by shifting the envelope of turbine rig noise, which

includes all the engine turbine operating conditions, along
the abscissa by an amount equal to the area ratios of the
engine and rig nozzles which corrects for contraction ratio
giving an arbitrary but common velocity parameter. Two things
can be deduced from this crude assessment, the first is that
the noise being considered in this test was not jet mixing noise
and therefore could not be expected to correlate by using
normalising functions related to jet mixing noise, and secondly
that the important velocity parameter is not that of the jet
but some internal velocity. Such observations must lead to conjec-
ture about the effects of containing a noise source, particularly
on the velocity power index if this is to be used as a parameter
to distinguish sources. Theoretically the problem of a
turbulent noise generating region contained in an infinite
pipe has been investigated by Davies and Ffowcs Williams (9).
In the analysis it is established that the velocity index
is unmodified for high acoustic frequencies or turbulence source
regions which are not correlated across the pipe, although a
reduction of 2 may be expected for sources which have
correlated turbulence or where only the plane wave mode of
propagation is excited. Similar results may be established for
dipole and monopole sources contained. In a further study (10)
Ffowcs-Williams considered the effect of a nozzle termination of
a low frequency incident wave to show that for moderate contraction
ratios of the kind seen in engines, the velocity index is increased
by two, whilst at the higher contraction ratios no further
modification is seen. Taking these results together gives the
qualitative result that the velocity index characteristics will

not be modified by containment in the jet pipe. Curle (11)
predicts U^6 sound from turbulent interaction with small
bodies, approximately the dependence often observed in tailpipe
noise. A turbojet has plenty of such bodies for example rear
bearing support struts or reheat systems operating in very
turbulent flow conditions.

Having established the possibility of tailpipe noise in
fact being generated upstream of the nozzle, it is worth
examining the effect of an acoustic absorber on this noise,
This has been done (Fig. 2.4) using the same engine used for the
comparison given in fig 2.2. but now the influence of angle
is seen at a condition corresponding to line C. The acoustic
absorber, which is of a perforate plate type, clearly gives an
attenuation, the angular range being very large (Fig. 2.5) even
well past the normal to the jet axis, so circumstantial
evidence leads to the conclusion that at least part of the tail
pipe noise emanates from within the engine.

Experiments using screens at the nozzle exit also tend to substantiate this conclusion, giving large reduction as shown in fig. 2.6. By reference to the insert sketches of the screen configurations, it is seen that the size of the screen is of secondary importance, so long as the region of the nozzle is covered to put the measuring point in shadow. This configuration would however effectively reduce any signal from the nozzle lip as well as disturbances from upstream. Efficient noise sources near edges are discussed by various authors. The influence of an edge on quadrupole radiation is shown by Levine (12) to greatly enhance the acoustic energy radiated as expressed below.

$$\text{acoustic energy} \sim \frac{Q_L^2}{64\pi\rho c^2 d^3} \frac{1 - \frac{M^2}{4}}{(1 - M^2)^{5/2}} \qquad M < 1$$

for a longitudinal quadrupole of strength Q_L a distance d from a refracting edge with flow Mach number M. This represents a sound scattering mechanism with intensity increasing in proportion to the fifth power of flow velocity, becoming more powerful as the primary source displacement 'd' decreases.

A similar problem of the scattered noise field due to an eddy interaction very close to a semi infinite plane as published by Ffowcs-Williams and Hall (13). Here it is shown that the resulting far field may be represented by

$$I \sim \frac{u^5}{(kr)^3} \, \text{Sin}^2\left(\frac{\theta}{2}\right)$$

where r is the characteristic distance of an eddy from the edge. The mechanism described produces noise of intensity greater than that due to the unbounded turbulence by a factor $(kr)^3$.

Crighton and Leppington (14) have generalised the work for various bodies which may be either rigid or considered acoustically soft.

The substance of the previous results survives which in terms
of intensity give $I \propto U^6$ for a hard body of dimensions less than
the acoustic wavelength, modified to $I \propto U^4$ for the soft body,
c.f Curle (11), whilst for the semi infinite wedge of angle $P\pi/q$
the result becomes $I \propto U^{4+2q/P}$ for both hard and soft surfaces c.f
Ffowcs Williams et al (13). It is argued in this work that
the problem of the singularity of the induced velocity at the
edge may be ignored. This concerns the length scale pertinent
to the region controlled by viscosity, and hence not within the
bounds of Lighthill's original assumption concerning the effect
of the turbulence induced field on the Reybold stress term.
This scale is much less than the acoustic wavelength for low
Mach number and high Reynolds number flows as encountered in
the practical problem. The particular aspects of the problem
associated with edge effects on the flow are investigated by
Crighton (12) where the noise due to reaction from an unsteady
shear layer on both rigid and compliant edges to the semi-
infinite plate, resulting in the following intensity prediction.

a) $\quad I \sim U^5 \sin^2\left(\frac{\theta}{2}\right)$ 　　For rigid plate without Kutta condition.

b) $\quad I \sim U^3 \csc^2\left(\frac{\theta}{2}\right)$ 　　For the corresponding full Kutta condition with the vortex sheet leaving the plate at zero gradient.

c) $\quad I \sim U^5 \sin^2\theta$ 　　For a compliant plate without Kutta condition.

For short wavelengths, these results may be used for the
circular orifice of jet nozzles. The long wave problem is
considered by Leppington (12) who shows similar characteristics
to the result obtained by Curle (11) for small bodies, now.

$$I \sim \frac{U^6}{kR} \sin^2\left(\frac{\theta}{2}\right)$$ 　　where 'R' is the pipe radius.

This is quite different to the previous results from semi infinite plate scatterers, being a much less efficient phenomenon with more characteristics of interaction with a small body than a semi infinite pipe.

Attempts to modify these sources at the edge by changing the character of the turbulence incident on the edge have produced interesting results as seen by experiments on the engine previously described in fig. 2.1., 2.2. The engine was built to incorporate a simple flow straightener constructed as a square honeycomb of ~3 cm cell size and ~15 cm depth. The resulting effect on spectra is quite dramatic as is seen from fig. 2.7 which represents the noise spectrum at 120° to the exhaust axis for three conditions previously shown. Which Fig. 2.8 shows the angular dependance of the phenomena, exhibiting a strong tendency towards angles greater equal to 90°, as expected from the theoretical models without full Kutta conditions. More evidence of the potential importance of edge scattering is seen from screening tests where increases in the high angle noise may be seen as the jet becomes closer so that "R_f" becomes small for turbulence in the mixing region, a result which is demonstrated in fig. 2.9 which compares attenuation field shapes for both close proximity and remote nozzle screens. The inserted $\frac{1}{3}$rd octave spectral comparasons for 105° to the axis indicate how the near screen tends to increase the low frequency noise and looses the high frequency attenuation seen with the remote screen.

THE EFFECT OF FORWARD SPEED

Motion of an acoustic source has a fundamental effect on both the spectral and field strength characteristic of that source. Spectral changes are due to the doppler shift of frequency.

Field strength changes depend upon the source type involved and may be briefly summarised by the use of an amplification term of $(1 - M_s \cos\theta)^{-N}$ on the basic source strength. In this case, for isolated sources 'M' has the value 4 for monopole and dipole sources, and 6 for quadrupoles when considering the far field intensity. This ensures that the source strength remains constant with the motion, a situation not expected for jet noise where the shear stress is though to change with jet relative velocity.

To illustrate this, fig. 3.1. A and B reproduced from figs. 1.1. now includes information from flight tests. These data are presented in two ways, the first plotted as a function of exit jet velocity, and the second as a function of relative jet velocity (in this case a mean line only is drawn to avoid confusion). For the low angle case the relative velocity model works quite well at the highest jet velocities, but starts to diverge as U_j decreases into the internal noise regime suggesting that jet noise is no longer dominant. However the reverse is true when using the absolute jet velocity model. At the high angles the absolute model gives good agreement but this is already considered to be more in the regime of tailpipe noise, so it is clear that some cross over must occur.

Comparisons of the static and in flight field shapes are illuminating, these are presented in fig. 3.2. for a flight engine and for a model nozzle. The latter being tested on the Rolls-Royce Spinning rig facility (Fig. 3.3) which consists of rotor arm with a tip jet propulsion unit. The field shapes demonstrate relative velocity reduction of the jet noise at the low angles, but the high angle noise is increased. This is considered to be due to source convection, not of the eddies in the jet now which are always travelling in the reverse direction with respect to the nozzle, but of aerodynamic sources outside and moving with the nozzle. Such sources in isolation can clearly be seen to suffer source amplification of the order $(1- M_A \cos \theta)^N$ which has previously been discussed. In this case M_A is the aircraft Mach number.

The example taken in fig. 3.2. takes the case of a super critical jet, where it is thought that amplification of the shock cell sources takes place, but other sources of tailpipe noise will suffer the same kind of amplification effects.

Rolls-Royce are actively persuing research into flight effects, which will be the subject of later publications.

References

1. Lighthill, M.J.
    On sound generated aerodynamically.
    I. General Theory
    Proc. Roy. Soc. A211, 1952.

2. Lighthill, M.J.
    On sound generated aerodynamically.
    II. Turbulence as a source of sound
    Proc. Roy. Soc. A222, 1954.

3. Ffowcs-Williams, J.E.
    Some thoughts on the effects of aircraft motion and eddy
    convection on noise from air jets.
    U.S.A.A. Report 155.   1960.

4. Ffowcs-Williams, J.E.
    The noise from turbulence convected at high speed.
    Phil. Trans. Roy. Sec. 1061, 255. 1963

5. Hoch, R.G. Duponchel, J.P., Cocking, B.J. and Bryce, W.D.
    Studies of the influence of density on jet noise.
    Paper presented at the First International Symposium on Air
    Breathing Engines,
    Marseille 19-23 June 1972.

6. Fisher, M.J.
    Analysis of Shock Associated Noise
    (Paper awaiting publication)

7. Ffowcs-Williams, J.E.
    Jet noise at very low and very high speed
    Proc. AFOSR-UTIAS Symposium, Toronto (May 1968)

8. Bushell, K.W.
    Some recent developments in low velocity and co-axial jet noise.
    Journal of Sound and Vibration 17(2) (1971)

9. Davies, N.G. and Ffowcs-Williams, J.E.
    Aerodynamic Sound Generation in a Pipe
    Journal of Fluid Mechanics (1968) Vol 32 Pt 5 (1968)

10. Ffowcs-Williams, J.E.
    Transmission of low-frequency jet pipe sound through a
    nozzle flow.
    Lecture to von Karmen Institute of Fluid Dynamics.
    Series 36. Turbulent jet flows (1971).

11. Curle, N.
    The influence of solid boundaries upon aerodynamic sound.
    Proc. Roy. Soc. A 231

12. Report of the ARC Working Party on Novel Aerodynamic
    Noise source Mechanisms at low jet speeds.
    Aeronautical Research Council, Noise Research Committee
    Report A.R.C. 32 925 May 1971.

References (continued)

13. Ffowcs-Williams, J.E. and Hall, L.H.
    Aerodynamic sound generation by turbulent flow in the
    vicinity of a scattering half-plane.
    Journal of Fluid Mechanics Vol 40 pt 4 (1970)

14. Crighton, D.G. and Leppington, F.G.
    On the scattering of aerodynamic noise.
    Journal of Fluid Mechanics, Vol 46, pt 3 (1971)

JET NOISE CORRELATION 45° TO JET AXIS.

$$\text{OASPL} - 10 \text{ LOG.} \left\{ \frac{\rho_J \, \rho_d}{\rho_o^2} \left(\frac{C_d}{C_o} \right)^4 \frac{A_J}{R^2} \right\}$$

□ ROLLS ROYCE MODEL NOZZLES
× ROLLS ROYCE ENGINES

$$\text{LOG.} \frac{V_J}{C_d}$$

FIG. 1.1A.

JET NOISE CORRELATION ~ 105° TO AXIS.

$$\text{OASPL} - 10 \, \text{LOG} \left\{ \left[\frac{\rho_J \, \rho_d}{\rho_o 2} \left(\frac{C_d}{C_o} \right)^4 \frac{A_J}{R^2} \right] \right\}$$

SHOCK CELL
NOISE REGION

⊙ ⊡ ROLLS ROYCE MODEL NOZZLES
× ROLLS ROYCE ENGINES
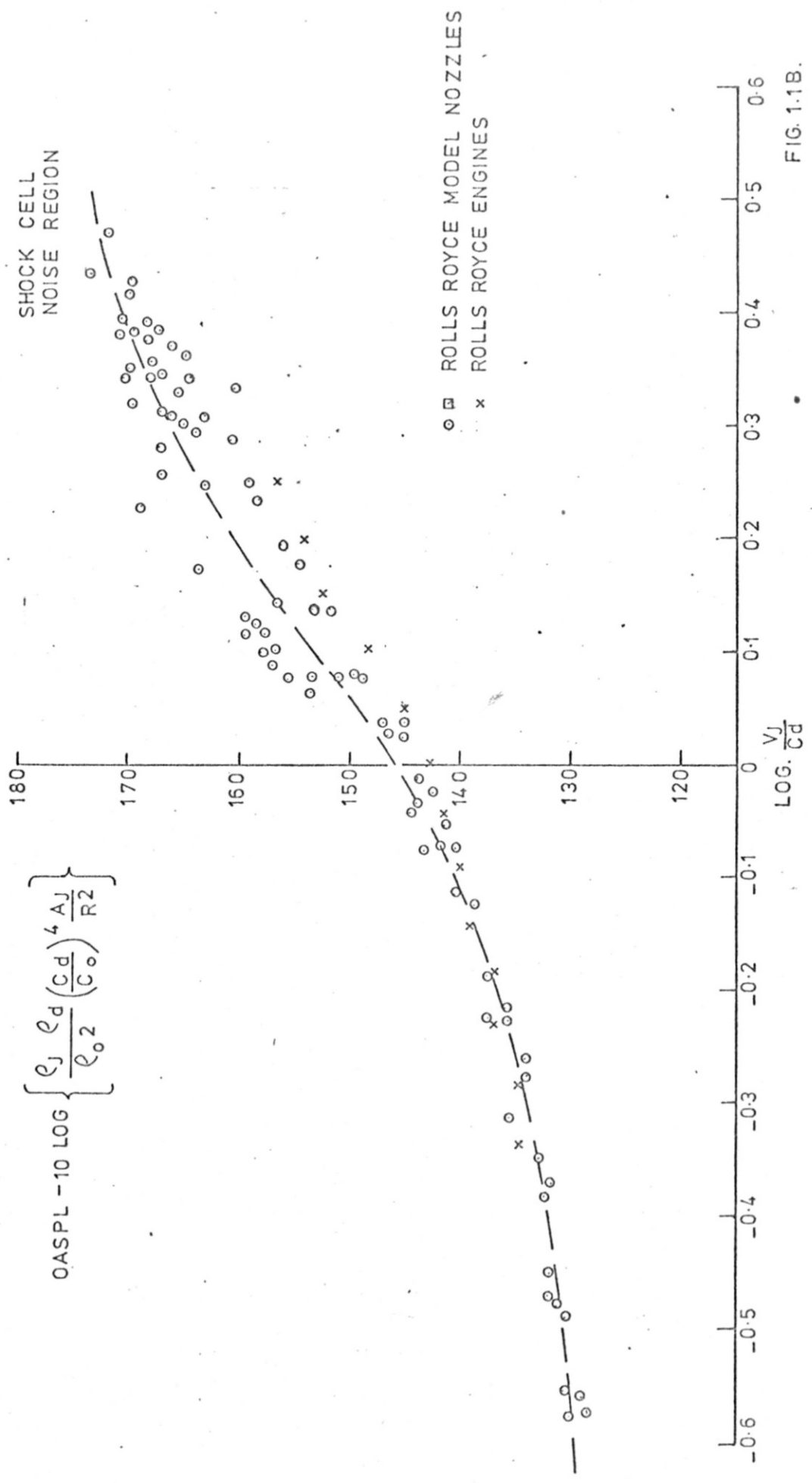
LOG. $\frac{V_J}{C_d}$
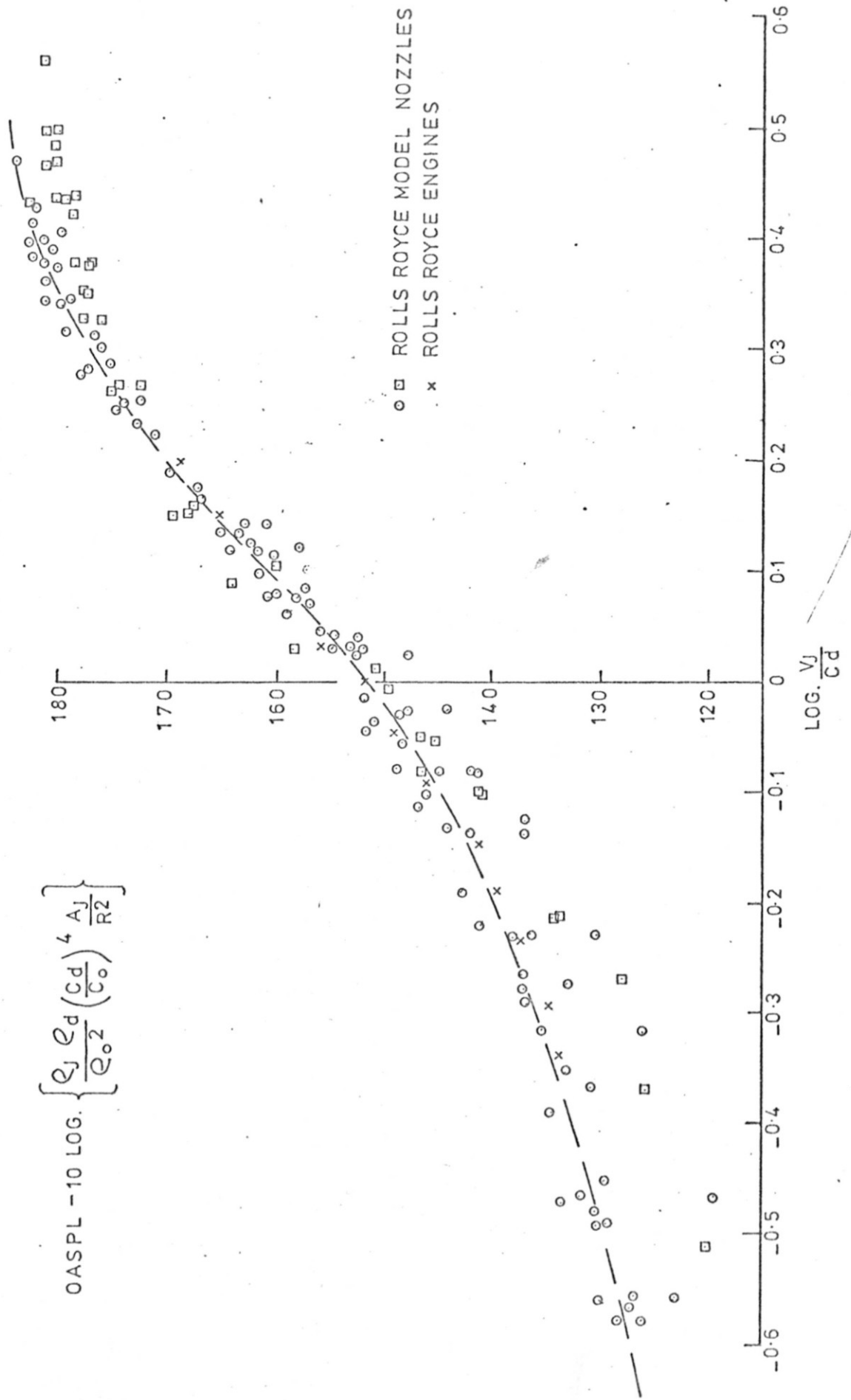
FIG. 1.1B.

LINEAR FIELD SHAPES FOR CONICAL, CON-DI, AND PERFORATED SHROUD NOZZLE CONFIGURATIONS.

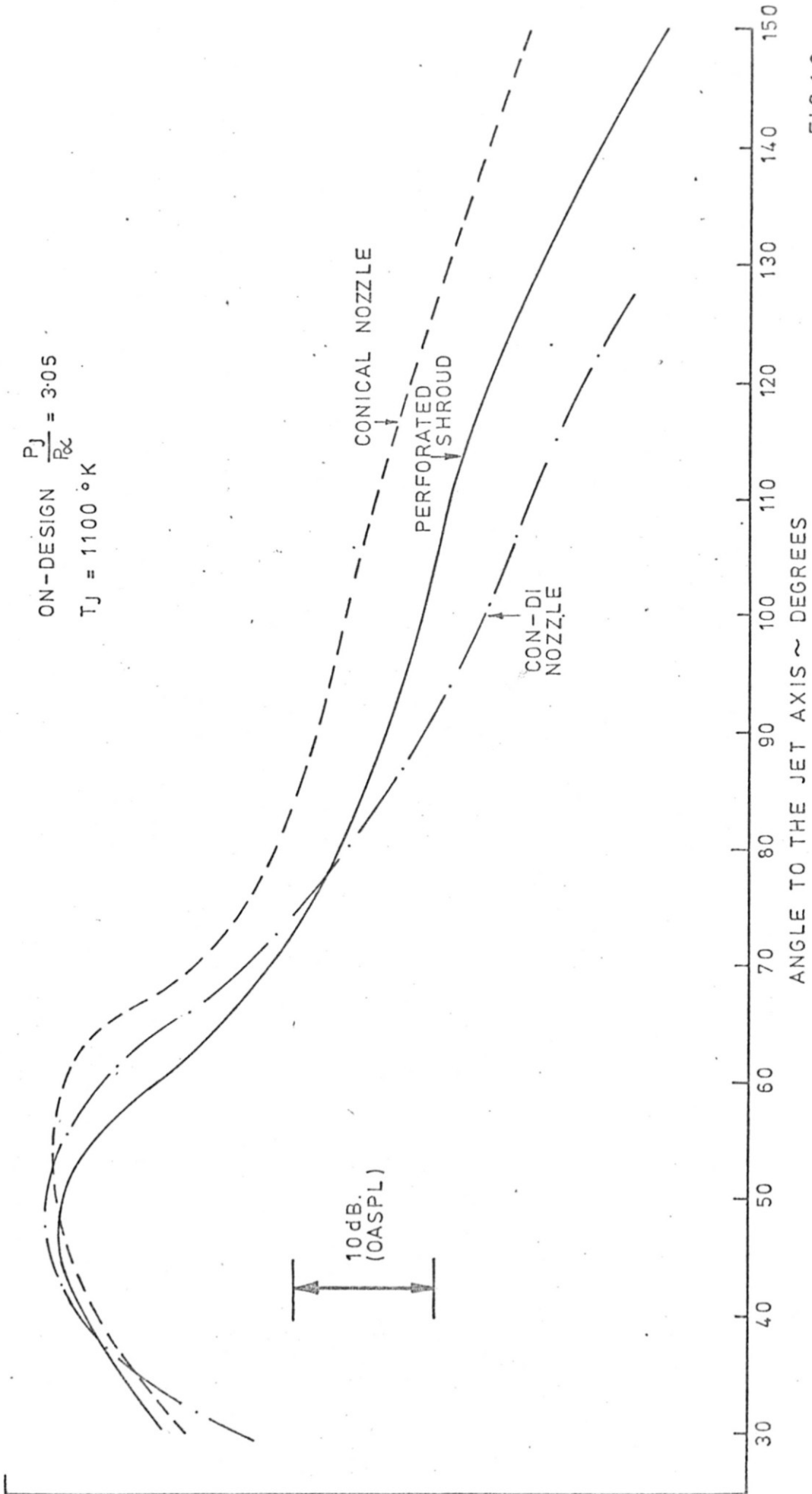ON-DESIGN $\frac{P_J}{P_\infty}$ = 3·05

T_J = 1100 °K

CONICAL NOZZLE

PERFORATED SHROUD

CON-DI NOZZLE

10 dB. (OASPL)

ANGLE TO THE JET AXIS ~ DEGREES

30   40   50   60   70   80   90   100   110   120   130   140   150

FIG. 1.2.

COMPARISON OF PERFORATED SHROUD WITH CONICAL AND CON-DI NOZZLE.

θ = 90°

10 dB.

○ PERFORATED SHROUD
△ CON-DI NOZZLE
× CONICAL NOZZLE

θ = 120°

10 dB.

ON-DESIGN $\frac{PJ}{P_\alpha}$ = 3·05

TJ = 1100 °K

θ = 150°

10 dB.

·5   ·8   1·25   2   3·15   5   8   12·5   20   31·5   50   K.HZ
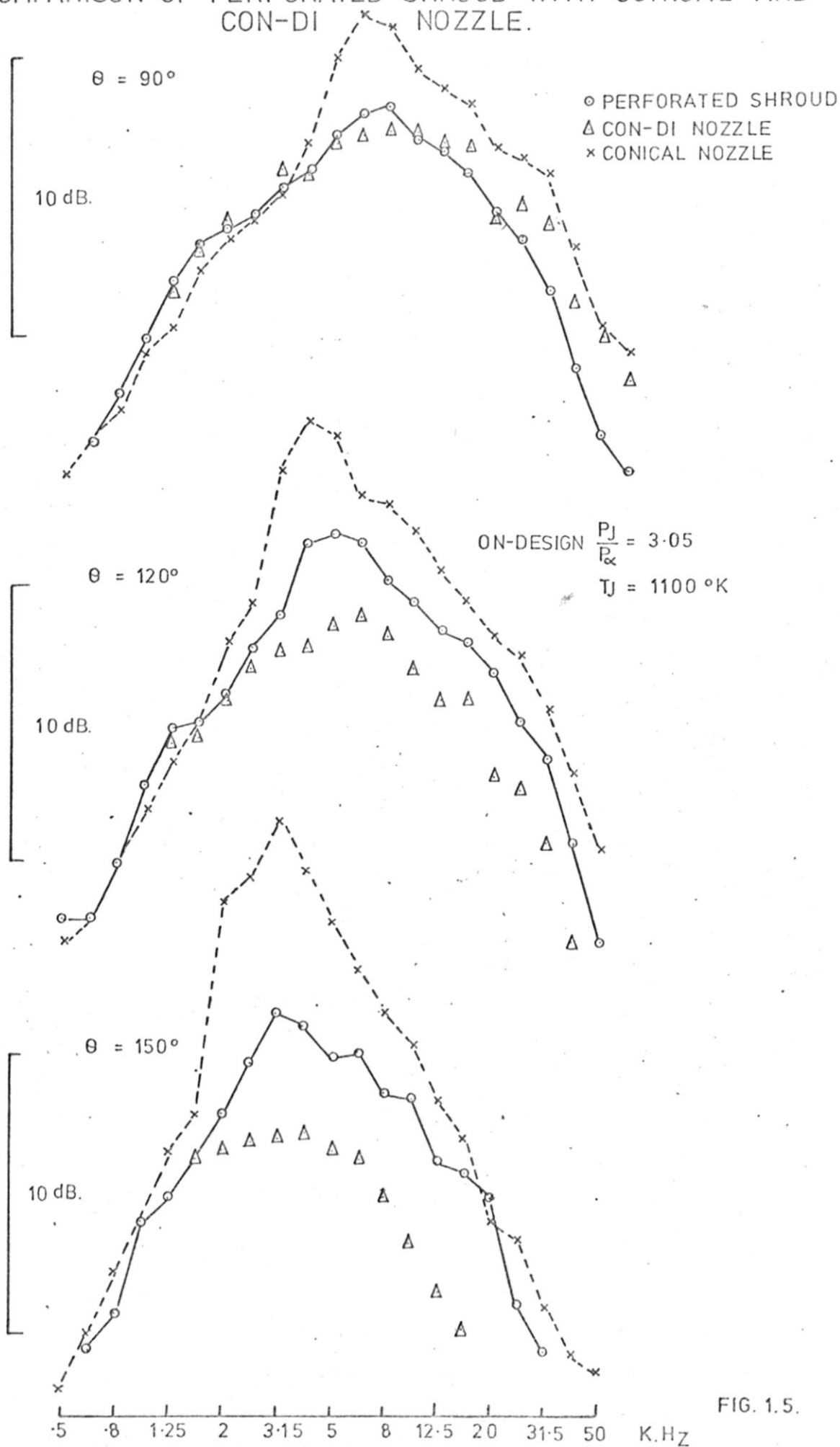
FIG. 1.5.

LINEAR ACOUSTIC FIELD SHAPE, WIDE CONVERGENT PLATES WITH RESPECT TO
CONVERGENT NOZZLE.

5 PNdB.

—————— WIDE PLATES WITH EXIT PLANE VERTICAL
- - - - - WIDE PLATES WITH EXIT PLANE HORIZONTAL
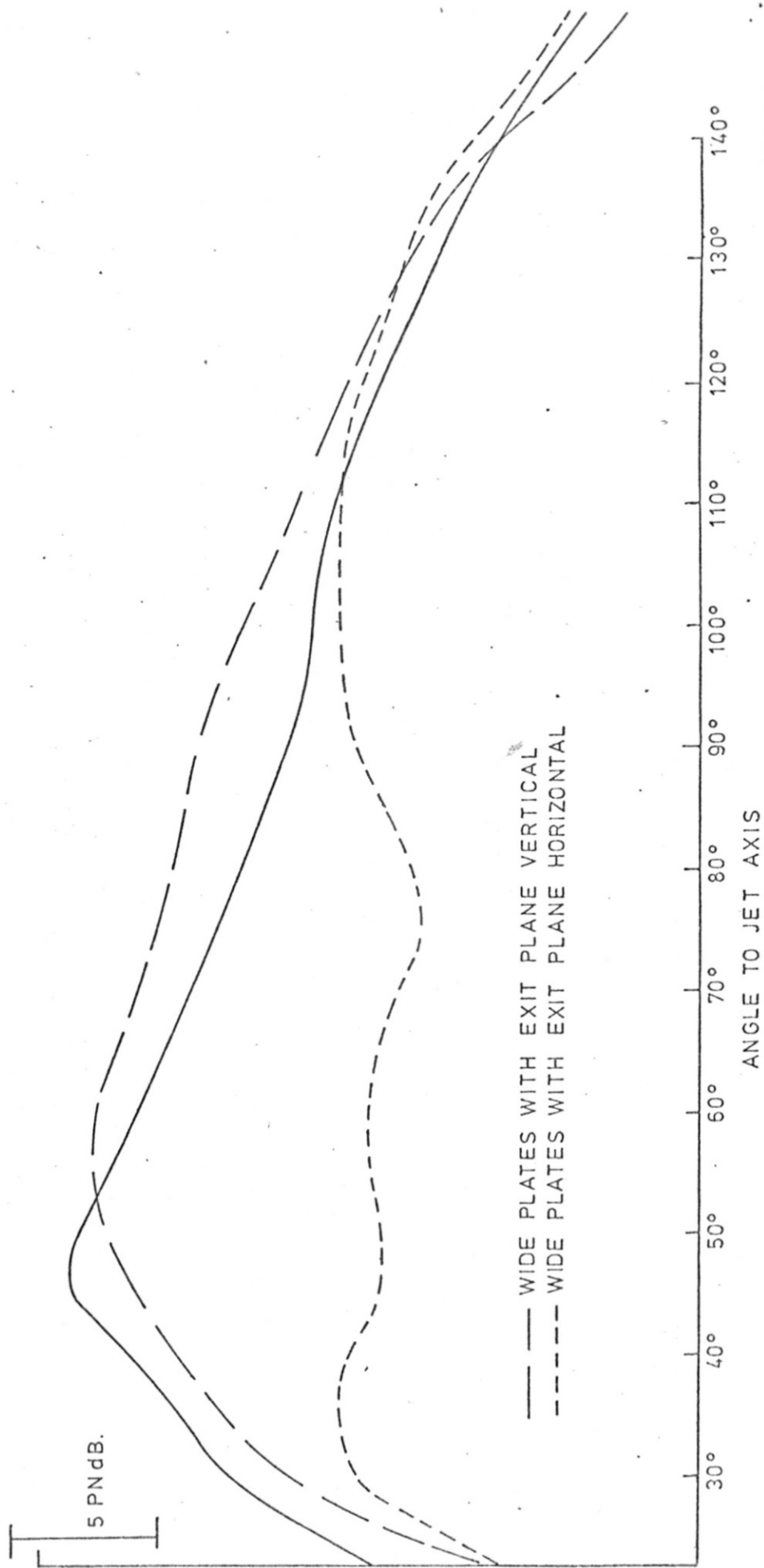
30° 40° 50° 60° 70° 80° 90° 100° 110° 120° 130° 140°

ANGLE TO JET AXIS

FIG. 1.9.

VARIATION OF PLATE SEPARATION ON SQUASHED JET
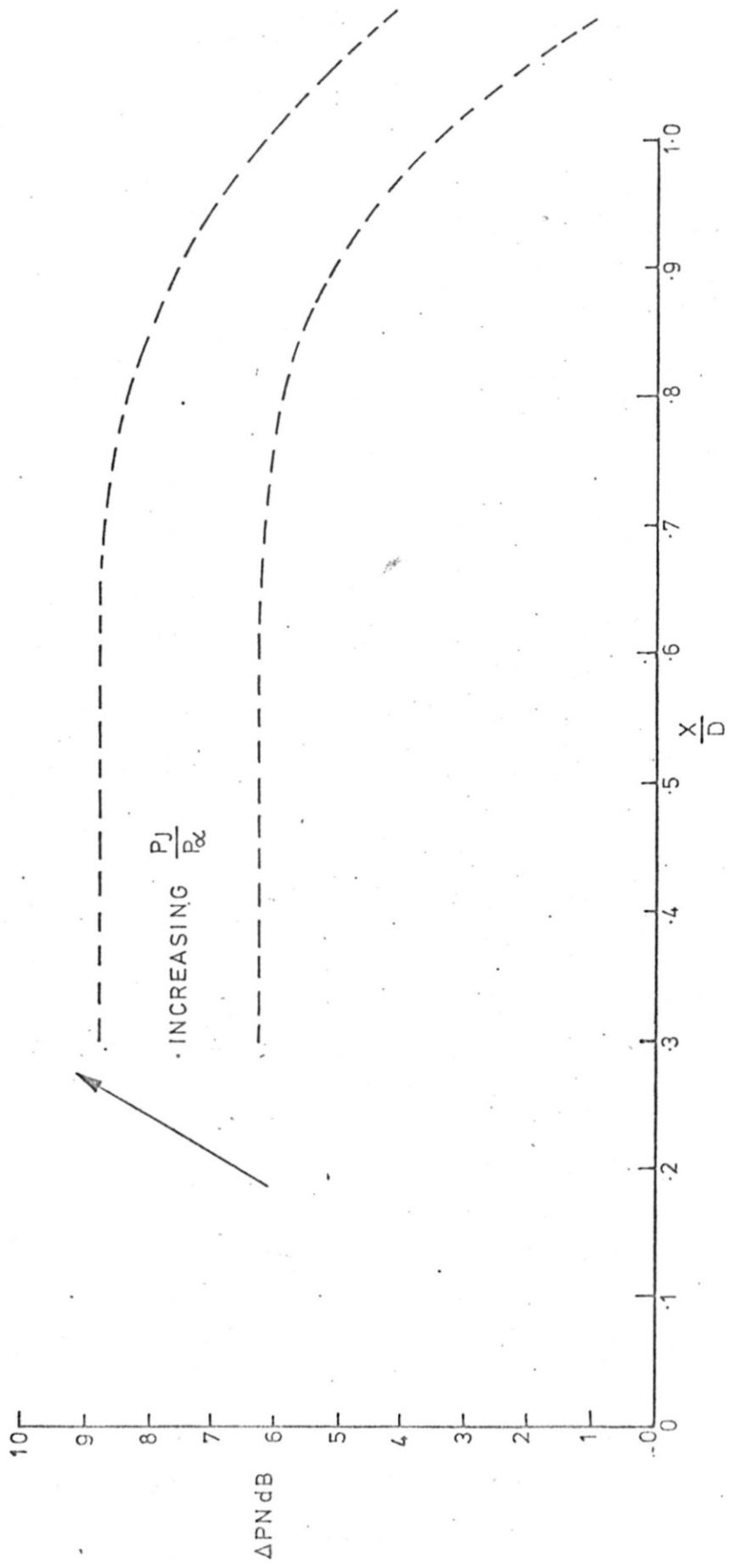(PEAK TO PEAK ATTENUATION RELATIVE TO CONICAL DATUM NOZZLE)

INCREASING $\dfrac{P_J}{P_\infty}$

ΔPNdB

$\dfrac{X}{D}$

FIG. 1.10.

TWIN-NOTCH NOZZLE FIELD SHAPE.

$\dfrac{P_J}{P_\alpha} = 3\cdot25 \qquad T_J = 1100\,^\circ K$
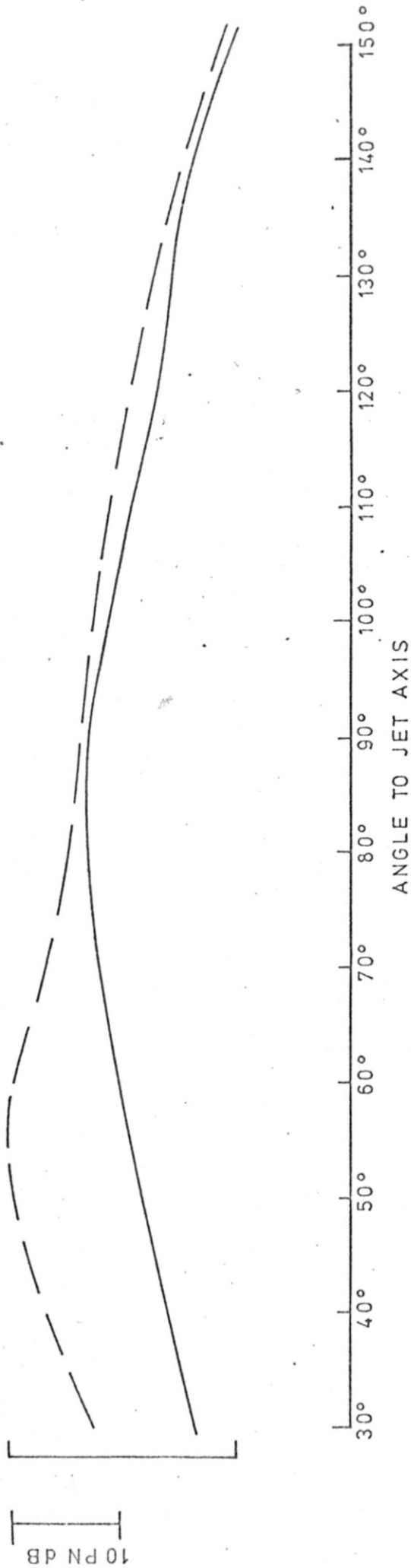
FULL SCALE (EXTRAPOLATION)
——————— TWIN NOTCH
— — — — CONICAL DATUM

10 PN dB

30° 40° 50° 60° 70° 80° 90° 100° 110° 120° 130° 140° 150°

ANGLE TO JET AXIS

FIG. 1.13.

CORRELATION OF NOISE AT 90° TO JET AXIS.

$$\text{OASPL} - 10 \, \text{LOG}_{10} \left[\left\{ \left(\frac{C_\alpha}{C_o} \right)^4 \frac{A_J}{R^2} \left(\frac{\rho_J}{\rho_\alpha} \right)^3 \right\} \right]$$

MEAN STATIC ENGINE LINE $\omega^3 = 2$
MEAN STATIC ENGINE VARIABLE ω^3
PURE JET MODELS VARIABLE ω^3

LOG$_{10}$ VREL C_α
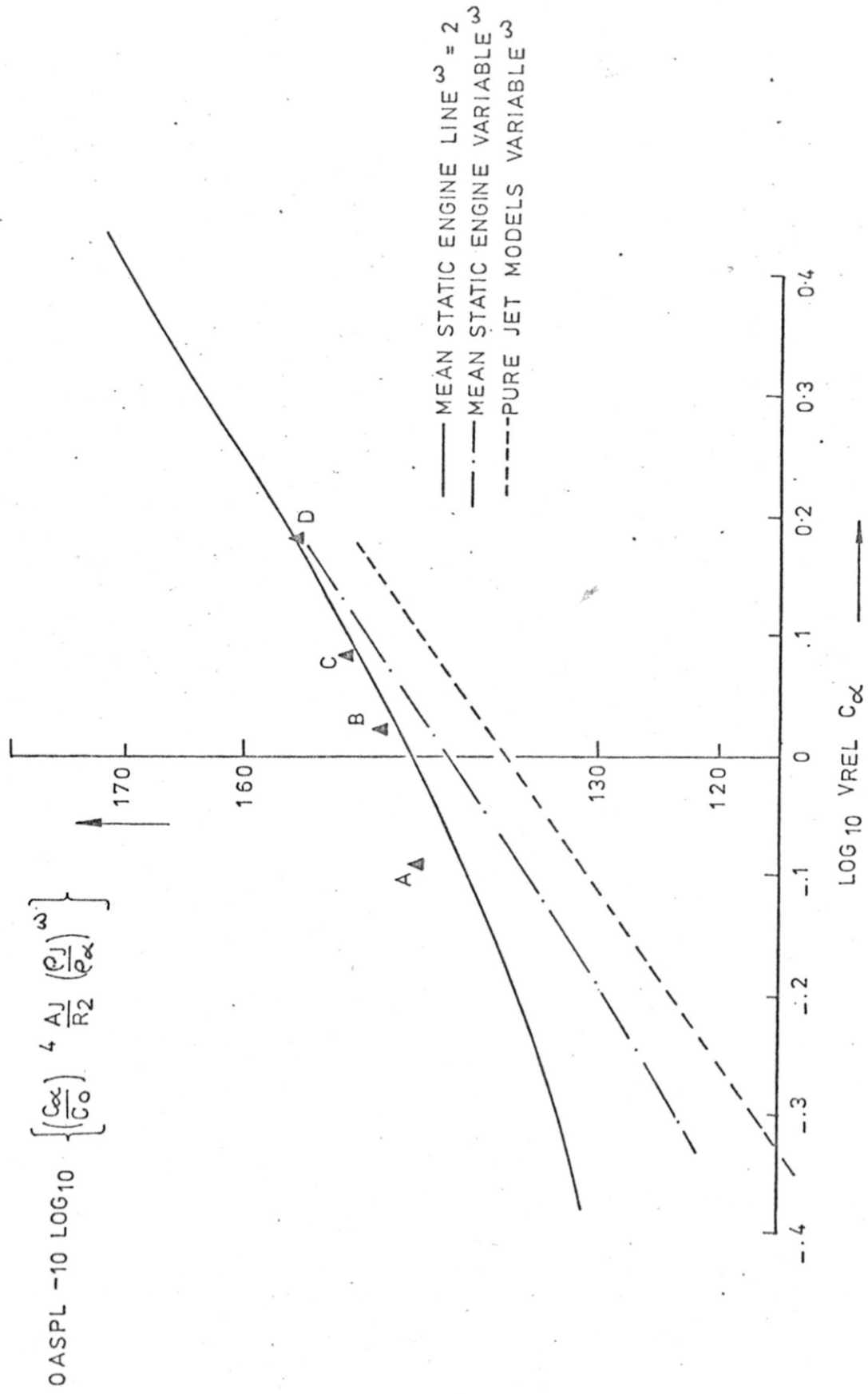
FIG. 2·1.

VARIATION OF NOISE WITH ENGINE SPEED 90° TO JET AXIS.

A V_J = 265 M/S
B V_J = 325 M/S
C V_J = 408 M/S
D V_J = 518 M/S

ESTIMATED JET NOISE FOR 'D'

LPT$_1$

HPT-LPT

3×LPC$_1$

HPT$_1$

D
C
B
A

2×LPC$_1$

ESTIMATED JET NOISE FOR 'A'

10 dB.

TYPICAL FILTER SHAPE @
32 Hz BANDWIDTH.

32 Hz BAND CENTRE FREQUENCY (KHZ)

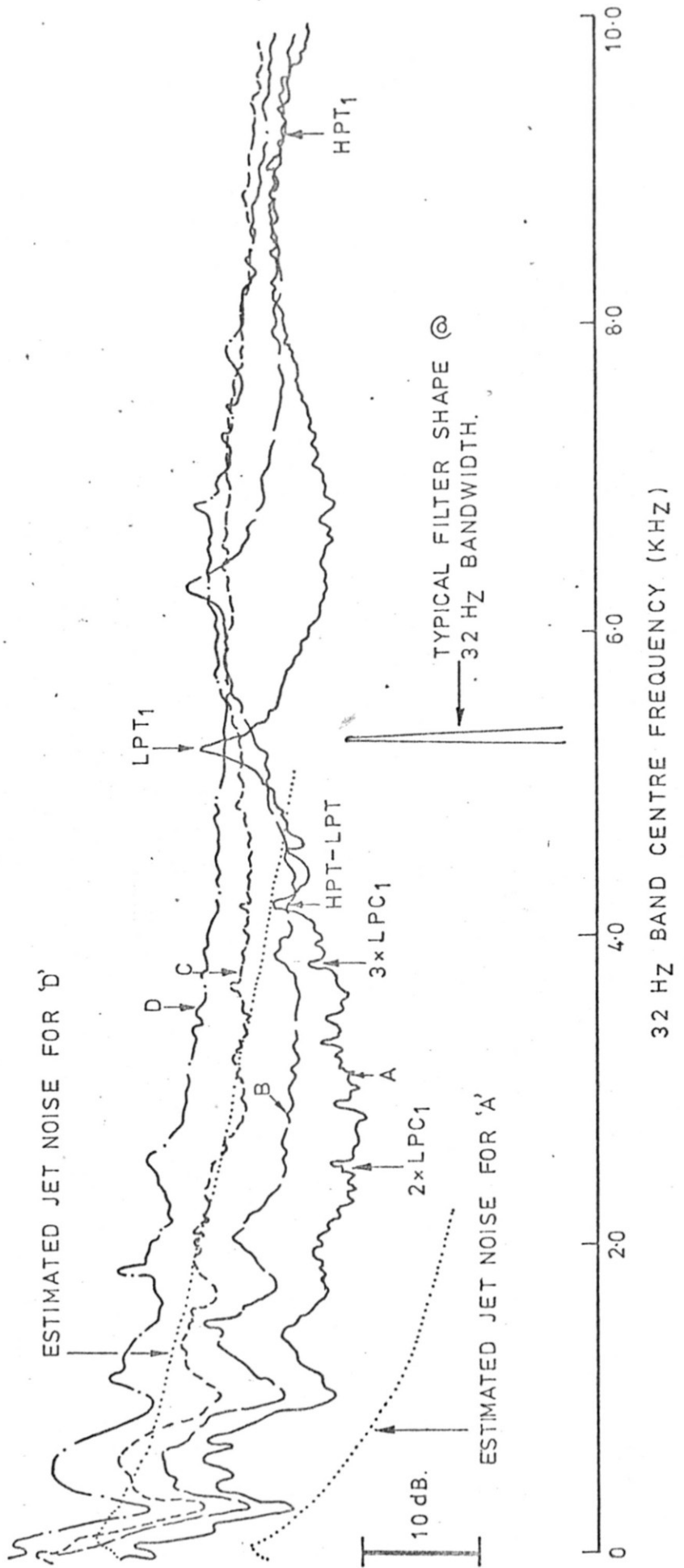0   2·0   4·0   6·0   8·0   10·0

FIG. 2.2.

CORRELATION OF TURBINE RIG NOISE AT 45°

$$\text{OASPL} + 10 \text{ LOG.} \left\{ \frac{P_J \; P_\alpha}{P_o{}^2} \left(\frac{C_\alpha}{C_o} \right)^4 \frac{A_3}{A_2} \right\}$$

ISOLATED TURBINE NOISE ENVELOPE
AS A FUNCTION OF RIG JET VELOCITY

TURBINE NOISE
A FUNCTION OF ENGINE
JET VELOCITY.

o   TOTAL NOISE OF ENGINE

□   TURBINE NOISE (DEDUCED
      FROM MEASUREMENT OF
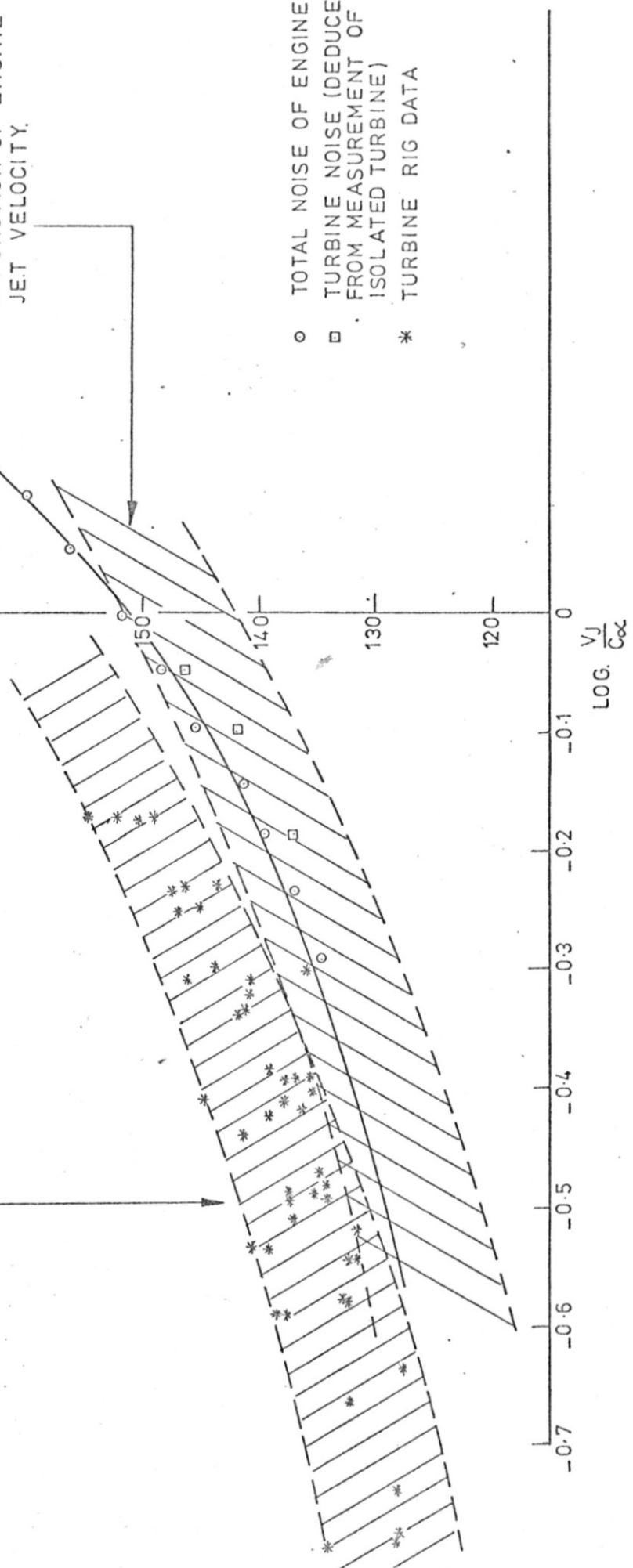   ISOLATED TURBINE)

*   TURBINE RIG DATA

LOG. $\frac{V_J}{C_\alpha}$

FIG. 2.3.

EFFECT OF JET-PIPE LININGS.

(CONDITION C. FIG. 2.2.)

—————— DATUM ENGINE
- - - - - - LINED JET PIPE

$\theta = 75°$

$\theta = 90°$

L.P.T. 1

DATUM ENGINE

LINED JET PIPE

S.P.L.

10 dB.

32 Hz BANDWIDTH CENTRE FREQUENCY ~ KHz
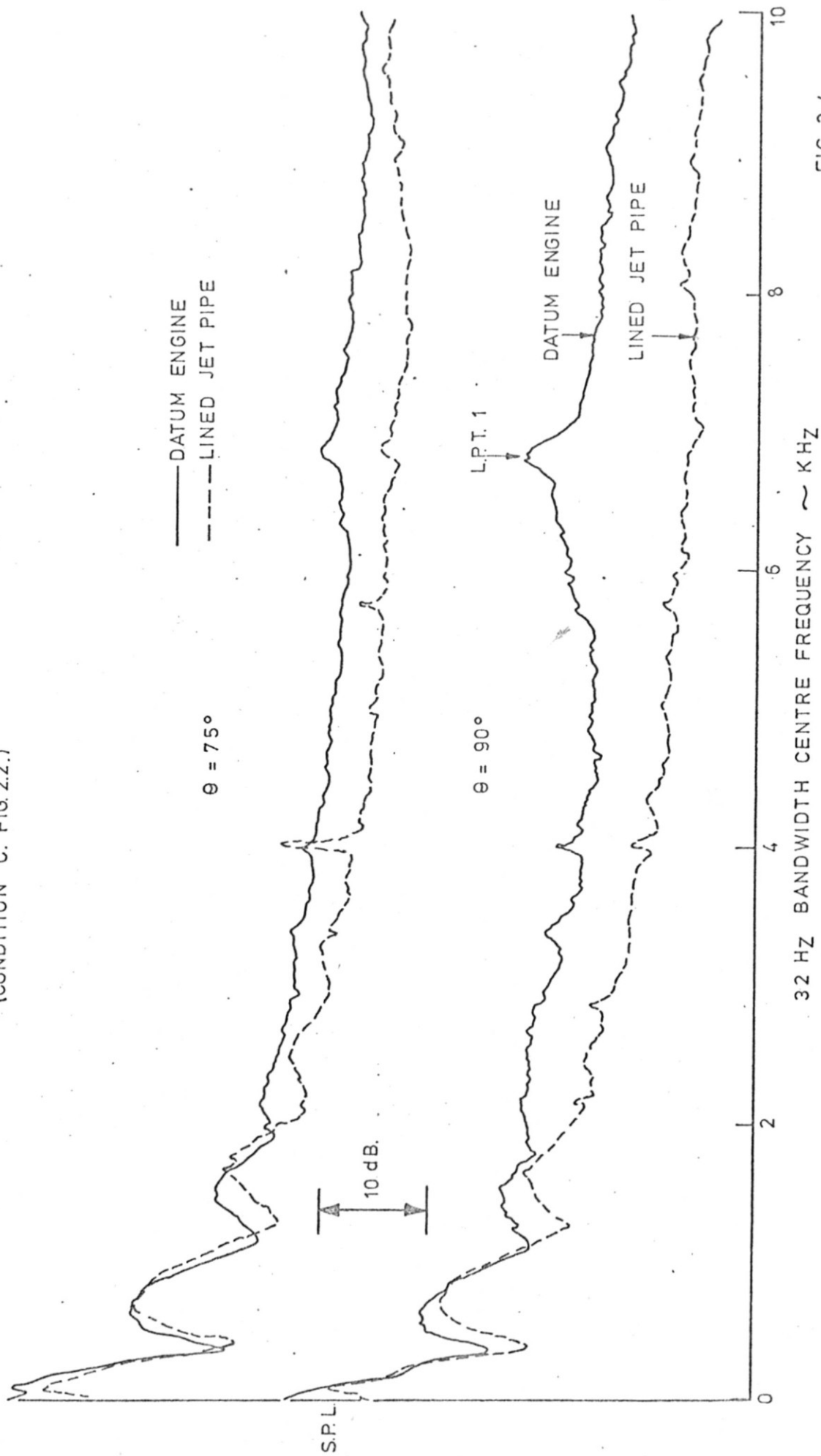
FIG. 2.4.

EFFECT OF ACOUSTICALLY LINED JET PIPE.

LINING
36 M AIR SPACE
23% POROSITY
1 MM. HOLE DIA.

45·7 M LINEAR

——— HARD JET PIPE
– – – LINED JET PIPE

Δ PN dB

10 PNdB

B

C

D

40 50 60 70 80 90 100 110 120 130 140

ANGLE TO THE JET AXIS
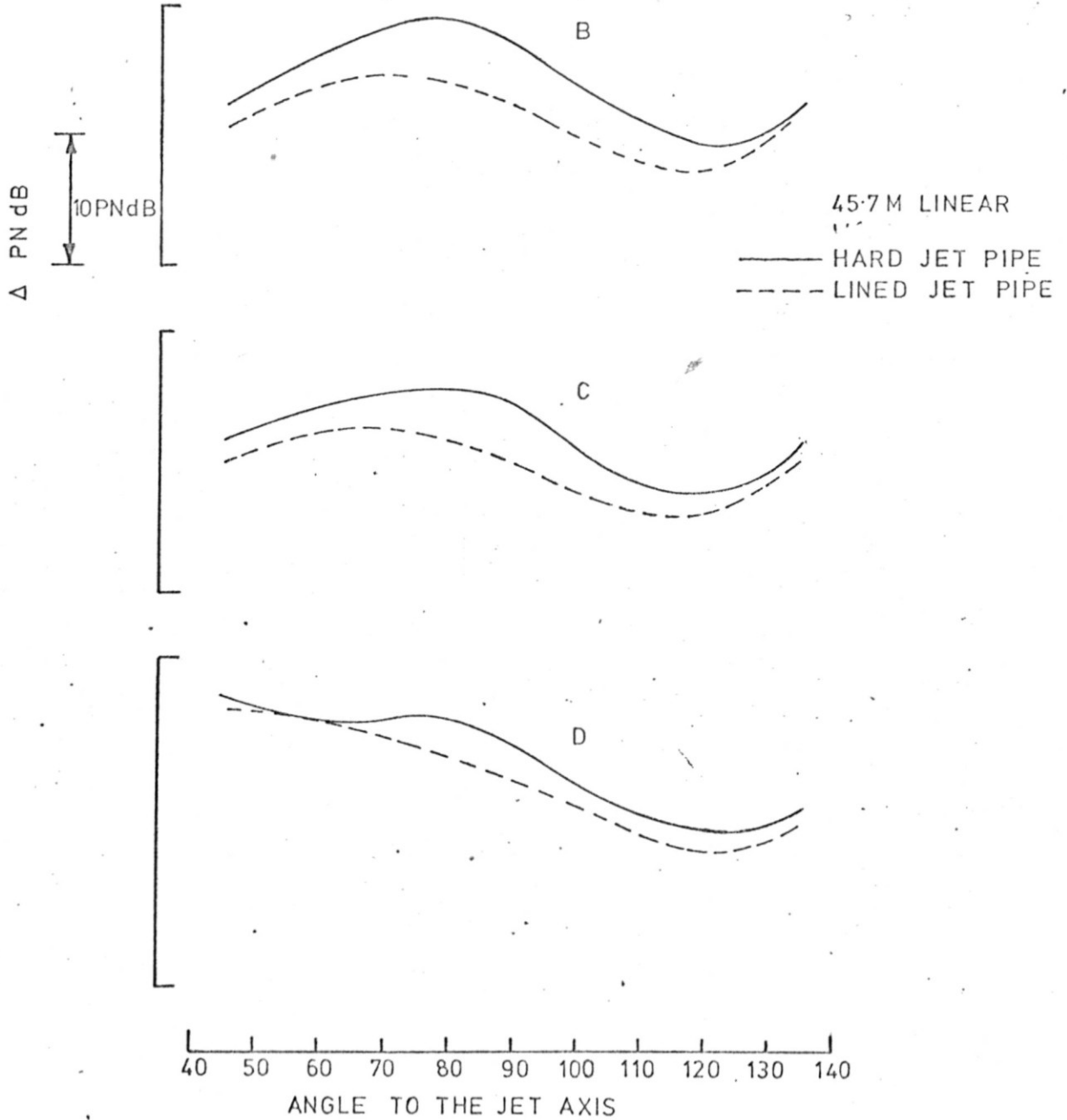
FIG. 2.5.

EFFECT OF SHIELDING THE NOZZLE.

SHIELD CONFIGURATION

① ——— DATUM ENGINE (RELATED TO ARBITRARY BASE LINE)

② —·—·— LARGE SCREEN (RELATED TO DATUM ENGINE ①)

③ ——— SMALL SCREEN (RELATED TO DATUM ENGINE ①)

17'

4.5'

4.5'

SIDE VIEW

TOP VIEW

32 Hz BANDWIDTH

θ = 90°

θ = 75°

SPL ~ dB.

10 dB

32 Hz BAND CENTRE FREQUENCY ~ (K Hz)

FIG. 2.6.

EFFECT OF EGG-BOX.

θ = 120° TO JET AXIS

① ——— DATUM ENGINE + INTAKE SCREEN
(RELATED TO ARBITRARY BASE LINE)

② ----- 'EGG-BOX' + INTAKE SCREEN

32 Hz BANDWIDTH
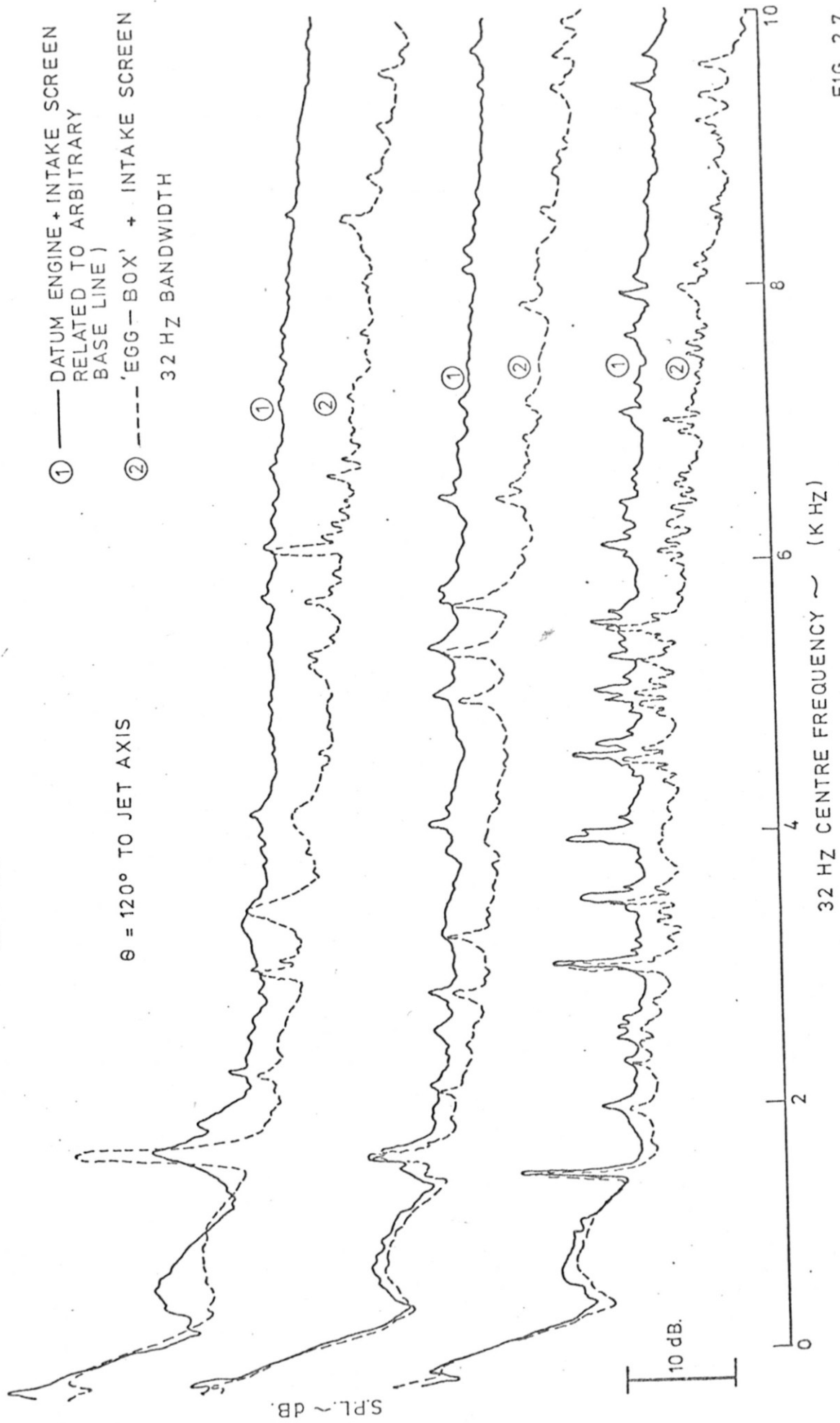
S.P.L.~ dB.

10 dB.

32 Hz CENTRE FREQUENCY ~ (KHz)
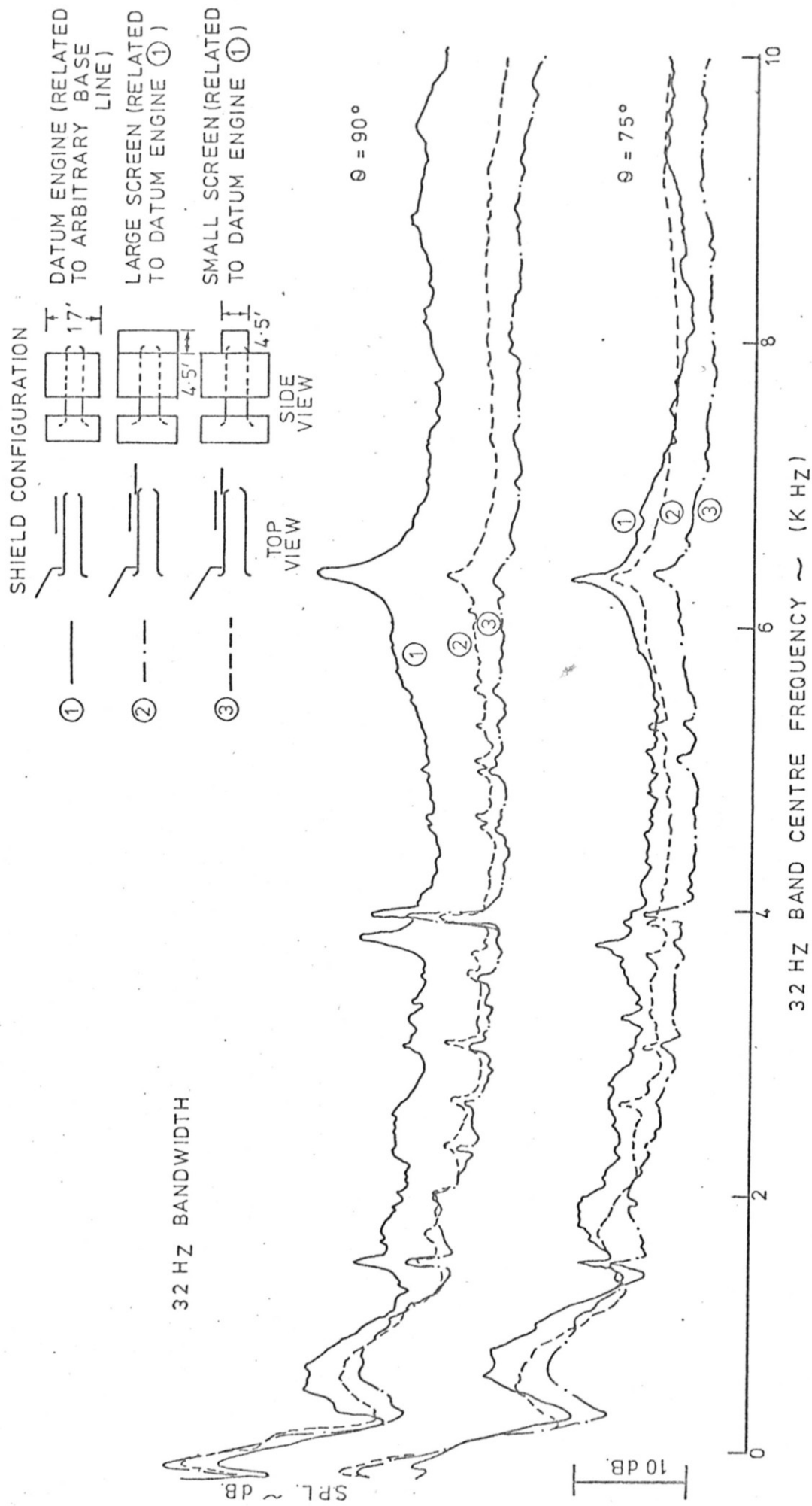
FIG. 2.7.

EFFECT OF θ ON ATTENUATION DUE TO EGG BOX.

CONDITION C. FIG. 2.2.

① ----DATUM ENGINE RELATED TO ARBITRARY BASE LINE.

② ——EGG BOX RELATED TO ①

θ = ANGLE TO JET AXIS.

θ = 135°

θ = 120°

θ = 90°

θ = 75°

3×LPC1

2×LPC1

LPC1

LPC1

10 dB.

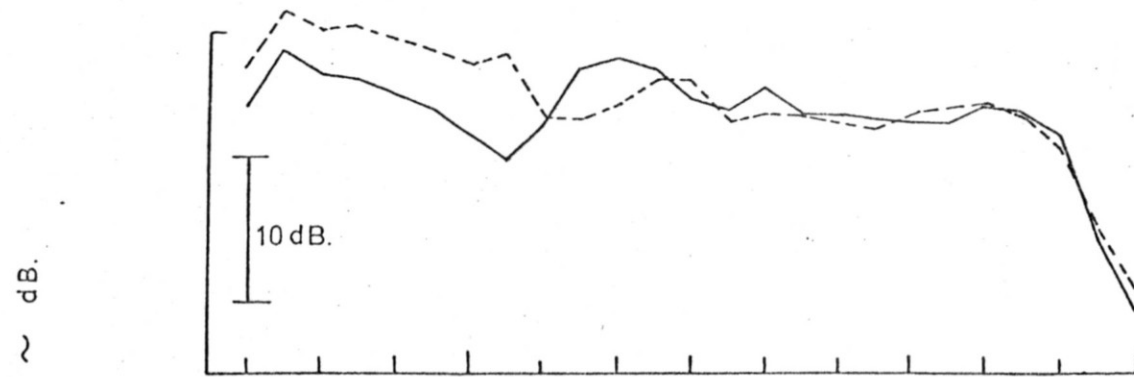2K   4K   6K   8K   10K

32 Hz BAND CENTRE FREQUENCY

FIG. 2.8.
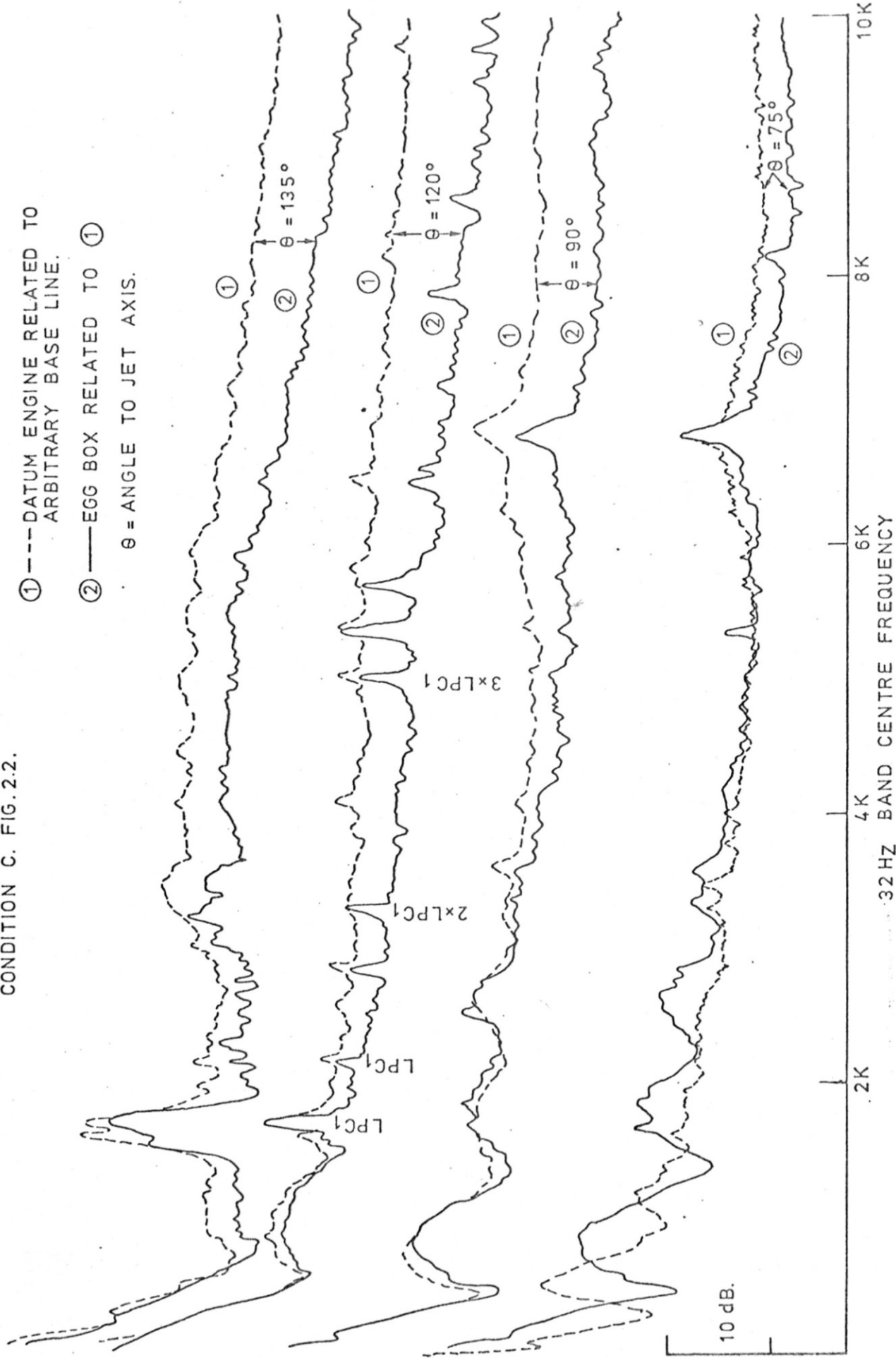
ATTENUATION FIELD SHAPE FOR NOZZLE SCREENS.
(FULL SCALE TENT)

ΔPNdB.

REMOTE SCREEN

CLOSE PROXIMITY SCREEN.

ANGLE TO JET AXIS
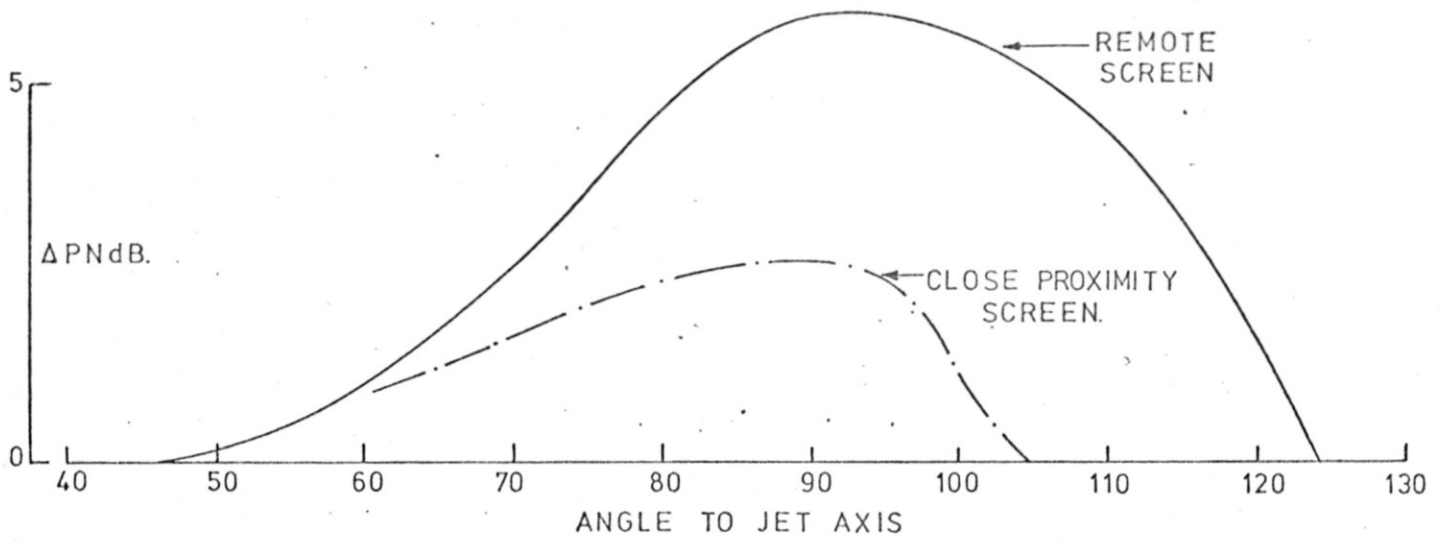
SPECTRAL EFFECT OF NOZZLE SCREENS
(θ = 105°)

CLOSE PROXIMITY SCREENS
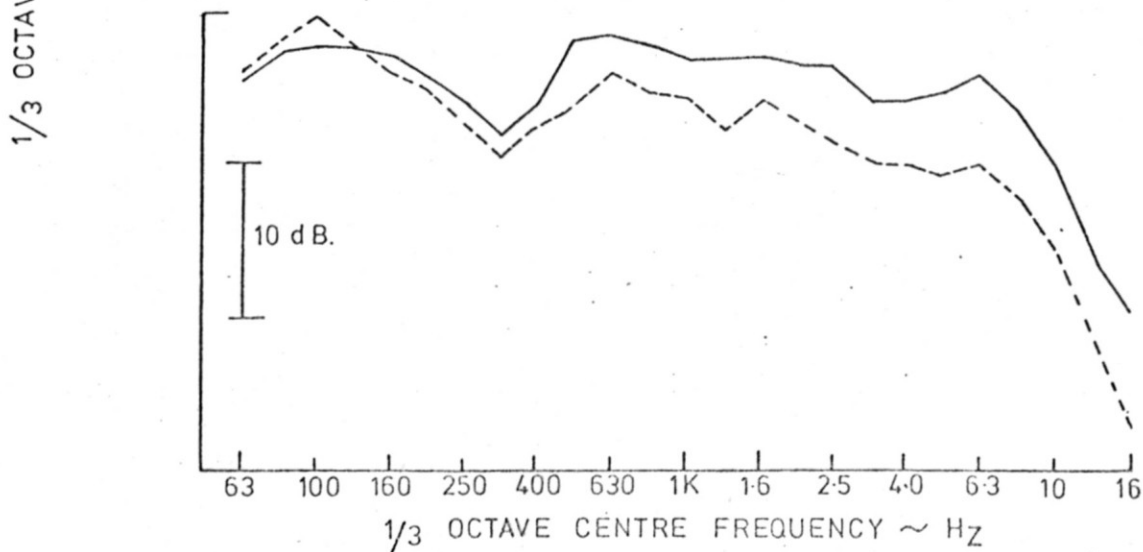
10 dB.

REMOTE SCREEN.

10 dB.

1/3 OCTAVE SPL ~ dB.

63   100   160   250   400   630   1K   1·6   2·5   4·0   6·3   10   16

1/3 OCTAVE CENTRE FREQUENCY ~ Hz

FIG. 2.9.

JET NOISE CORRELATION 45° TO JET AXIS.

$$\text{OASPL} - 10 \text{ LOG.} \left\{ \frac{\varrho_J \, \varrho_d}{\varrho_o^2} \left(\frac{C_d}{C_o} \right)^4 \frac{A_J}{R^2} \right\}$$

⊙ ROLLS ROYCE MODEL NOZZLES

⊡ ROLLS ROYCE ENGINES

× FLIGHT ENGINE VS. LOG V_J/C_α

+ FLIGHT ENGINE VS. LOG V_{REL}/C_α

FLIGHT ENGINE

LOG. $\frac{V_J}{C_d}$
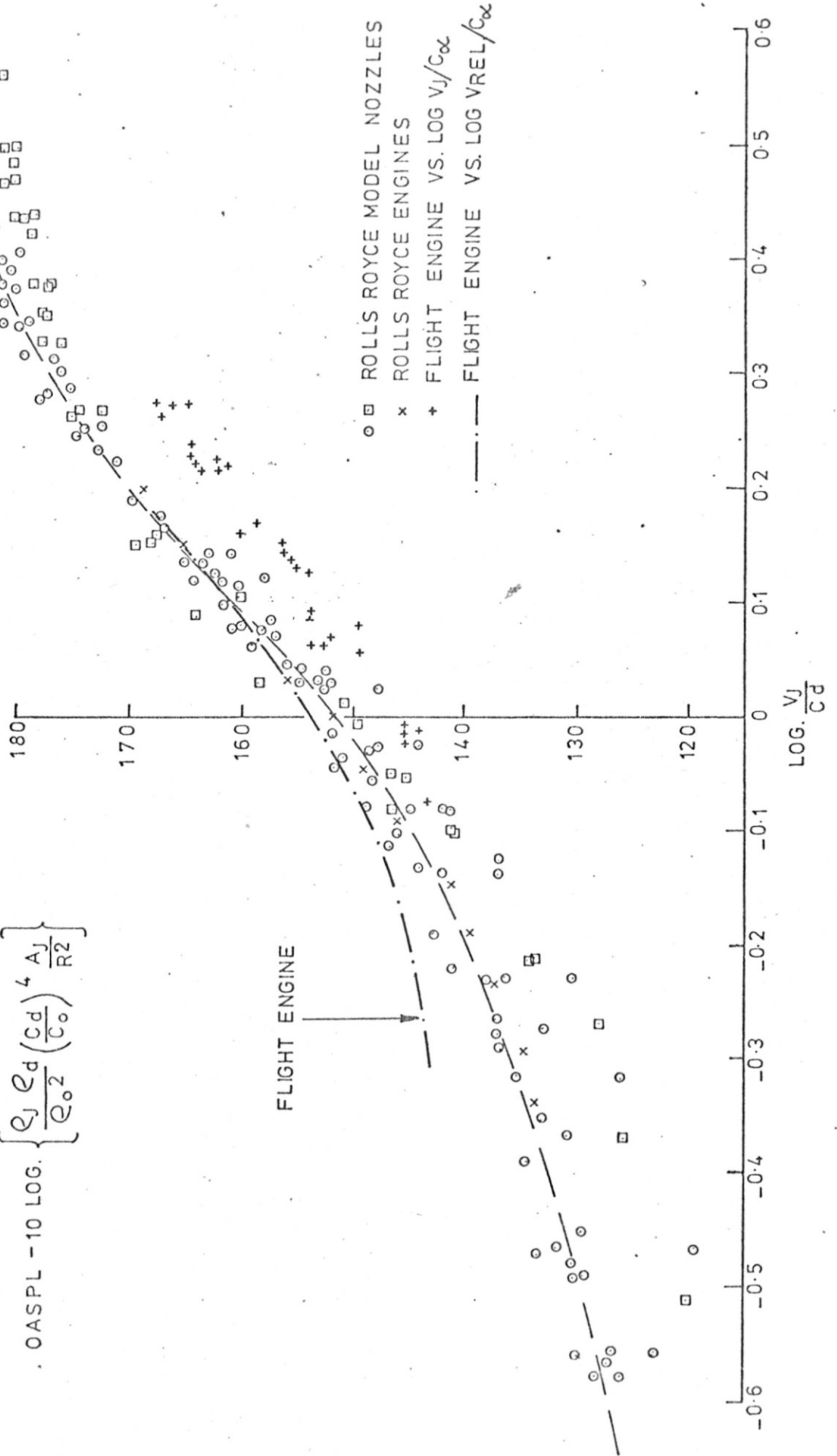
FIG. 3.1A.

JET NOISE CORRELATION ~ 105° TO AXIS.

$$\text{OASPL} - 10 \text{ LOG} \left\{ \frac{\rho_J}{\rho_o^2} \rho_d \left(\frac{C_d}{C_o}\right)^4 \frac{A_J}{R^2} \right\}$$

SHOCK CELL
NOISE REGION

FLIGHT ENGINE

LOG. $\frac{V_J}{C_d}$

⊙ ⊡ ROLLS ROYCE MODEL NOZZLES
×   ROLLS ROYCE ENGINES
+   FLIGHT ENGINE VS. LOG. V_J/C_α
—·— FLIGHT ENGINE VS. LOG. VREL./C_α
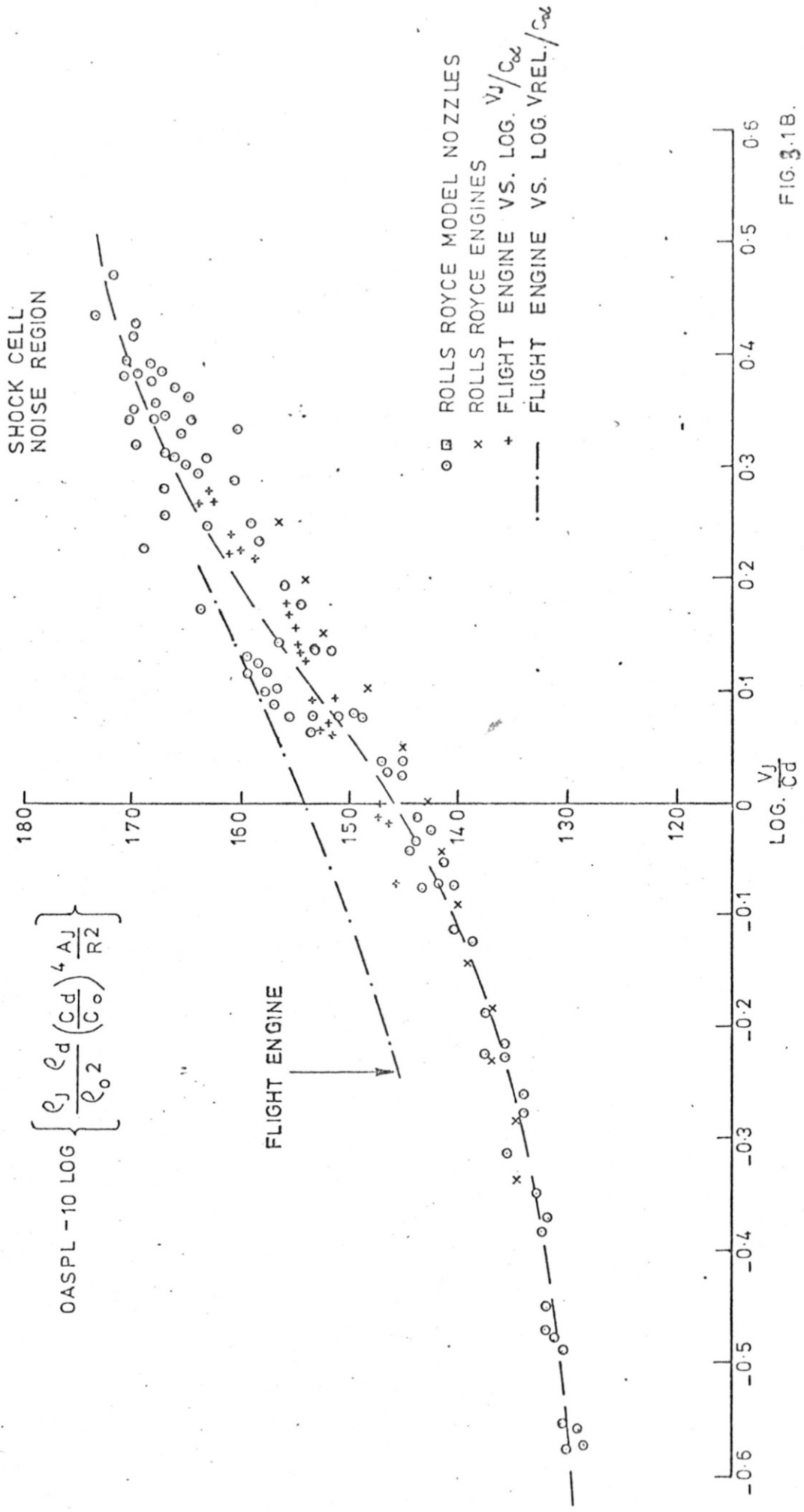
FIG. 3.1B.

EFFECT OF FORWARD SPEED ON DIRECTIVITY OF CHOKED CONICAL NOZZLE.

ENGINE

$PR = 2.5$ $T_J = 850°K$
$V_J = 2000$ FT SEC.
$V_F = 288$ FT SEC.
$(V_R = 1312$ FT SEC.$)$

N = FLIGHT MACH NO.

MODEL NOZZLE

$PR = 3.0$
$T_J = 1100°K$
$V_J = 2580$ FT S.

$V_F = 360$ FT/S.
$(V_R = 2220$ FT/S.$)$

STATIC

FORWARD SPEED

OASPL ~ dB.

5 dB.

STATIC

FORWARD SPEED

5 dB.

30   40   50   60   70   80   90   100   110   120   130   140

ANGLE TO THE JET AXIS ~ DEGREES

FIG. 3.2.